

---

# Gradients of Generative Models for Improved Discriminative Analysis of Tandem Mass Spectra: Supplementary Materials

---

**John T. Halloran**  
 Department of Public Health Sciences  
 University of California, Davis  
 jthalloran@ucdavis.edu

**David M. Rocke**  
 Department of Public Health Sciences  
 University of California, Davis  
 dmrocke@ucdavis.edu

## 1 Notation

| Symbol                       | Description   |
|------------------------------|---|
| $s$                          | observed spectrum of length $T$   |
| $m(s)$                       | observed spectrum precursor mass  |
| $c(s)$                       | observed spectrum precursor charge  |
| $O^{\text{mz}}$              | Observed peak m/z measurement   |
| $O^{\text{in}}$              | Observed peak intensity measurement   |
| $\mathcal{P}$                | set of all possible peptides  |
| $x$                          | peptide string, of length $n$ , comprised of amino acids, $x = x_1, x_2, \dots, x_n = x_{1:n}$  |
| $c(x)$                       | charge of peptide $x$ (note the overloaded use of the charge operator)  |
| $m(x_{1:t})$                 | mass of length- $t$ peptide $x_{1:t}$ (note the overloaded use of the mass operator)  |
| $\mathcal{D}$                | database of peptides to be searched   |
| $w$                          | mass tolerance threshold, used to filter peptides during search   |
| $D(s, \mathcal{D}, w)$       | candidate set of peptides to be scored and ranked in order to identify $s$  |
| $c_b$ and $c_y$              | b-ion and y-ion charge, respectively, such that $c_b = c_y = 1$ for $c(s) = 1$ and $c_b + c_y = c(s)$ for $c(s) > 1$ .  |
| $b(x, c_b, k), y(x, c_y, k)$ | $k$ th b- and y-ion pair of $x$   |
| $v$                          | length- $d$ theoretical spectrum of $x$   |
| $t$                          | arbitrary frame value for DRIP  |
| $\delta_t$                   | DRIP random variable signifying the number of theoretical peaks to move down in frame $t$ ; $\delta_t > 1$ corresponds to a deletion event  |
| $i_t$                        | DRIP Bernoulli random variable signifying whether an observed peak is scored as an insertion or not   |
| $K_t$                        | DRIP random variable signifying the theoretical peak index in frame $t$   |
| $a_{\text{mz}}$              | DRIP m/z insertion penalty  |
| $a_{\text{in}}$              | DRIP intensity insertion penalty  |
| $\mu^{\text{mz}}$            | vector of DRIP's m/z Gaussian means   |
| $\sigma^2$                   | DRIP's m/z Gaussian variance  |
| $\mu^{\text{in}}$            | DRIP's intensity Gaussian mean  |
| $\bar{\sigma}^2$             | DRIP's intensity Gaussian variance  |
| $\theta$                     | generative model's learnable parameters: for DRIP, this corresponds to all Gaussian means and variances; for Theseus and the modeled XCorr scoring function, this corresponds to the fragment ion weights |
| $\tau$                       | XCorr vector shift increment  |
| $z$                          | vector resulting from (XCorr) quantization and preprocessing of $s$   |
| $z'$                         | final step of XCorr preprocessing, where $z' = z - \sum_{\tau=-75}^{75} z_\tau$   |

|               |  |
|---------------|--|
| $z_\theta$    | reparameterized observed spectrum vector, such that a linear score may be computed as the product of $z_\theta$ and a boolean theoretical vector $u$ |
| $u$           | boolean theoretical vector with nonzero entries corresponding to the unity charge b-ions of $x$  |
| $M$           | set of discrete precursor masses, dictated by $w$ , iterated over in Theseus   |
| $X_{1:n}$     | random peptide modeled in Theseus  |
| $B_i$         | Theseus accumulated mass up to frame $i$   |
| $\mathcal{A}$ | set of amino acids   |
| $S_i$         | Theseus virtual evidence child in frame $i$  |

**Table 1:** Notation used in the main paper.

## 2 DRIP Fisher Score Derivation

Following the discussion in Section 3 of [2],  $\frac{\partial}{\partial \mu^{\text{mz}}(k)} \log p(s|x, \theta) = \frac{1}{p(s|x, \theta)} \frac{\partial}{\partial \mu^{\text{mz}}(k)} p(s|x, \theta)$  and we have  $\frac{\partial}{\partial \mu^{\text{mz}}(k)} p(s|x, \theta)$

$$\begin{aligned}
&= \frac{\partial}{\partial \mu^{\text{mz}}(k)} \sum_{i_{1:T}, \delta_{1:T}} p(i_{1:T}, \delta_{1:T} | \theta) = \sum_{i_{1:T}, \delta_{1:T}: K_t=k, 1 \leq t \leq T} \frac{\partial}{\partial \mu^{\text{mz}}(k)} p(i_{1:T}, \delta_{1:T} | \theta) \\
&= \sum_{i_{1:T}, \delta_{1:T}} \mathbf{1}_{\{K_t=k\}} \prod_{t: K_t \neq k} \phi(\delta_t, K_{t-1}, i_t, i_{t-1}) \frac{\partial}{\partial \mu^{\text{mz}}(k)} \prod_{t: K_t=k} \phi(\delta_t, K_{t-1}, i_t, i_{t-1}) \\
&= \sum_{i_{1:T}, \delta_{1:T}} \mathbf{1}_{\{K_t=k\}} \prod_{t: K_t \neq k} \phi(\delta_t, K_{t-1}, i_t, i_{t-1}) \left( \prod_{t: K_t=k} \frac{\phi(\delta_t, K_{t-1}, i_t, i_{t-1})}{p(O_t^{\text{mz}} | K_t)} \right) \left( \frac{\partial}{\partial \mu^{\text{mz}}(k)} \prod_{t: K_t=k} p(O_t^{\text{mz}} | K_t) \right) \\
&= \sum_{i_{1:T}, \delta_{1:T}} \mathbf{1}_{\{K_t=k\}} \prod_t \phi(\delta_t, K_{t-1}, i_t, i_{t-1}) \left( \prod_{t: K_t=k} \frac{1}{p(O_t^{\text{mz}} | K_t)} \right) \left( \frac{\partial}{\partial \mu^{\text{mz}}(k)} \prod_{t: K_t=k} p(O_t^{\text{mz}} | K_t) \right) \\
&= \sum_{i_{1:T}, \delta_{1:T}} \mathbf{1}_{\{K_t=k\}} p(s|x, \theta) \left( \prod_{t: K_t=k} \frac{1}{p(O_t^{\text{mz}} | K_t)} \right) \left( \frac{\partial}{\partial \mu^{\text{mz}}(k)} \prod_{t: K_t=k} p(O_t^{\text{mz}} | K_t) \right),
\end{aligned}$$

where

$$\begin{aligned}
\frac{\partial}{\partial \mu^{\text{mz}}(k)} \prod_{t: K_t=k} p(O_t^{\text{mz}} | K_t) &= \left( \prod_{t: K_t=k} p(O_t^{\text{mz}} | K_t) \right) \left( \sum_{t: K_t=k} \frac{\frac{\partial}{\partial \mu^{\text{mz}}(k)} \sum_{i_t=0}^1 p(i_t) p(O_t^{\text{mz}} | K_t, i_t)}{p(O_t^{\text{mz}} | K_t)} \right) \\
&= \left( \prod_{t: K_t=k} p(O_t^{\text{mz}} | K_t) \right) \left( \sum_{t: K_t=k} \frac{p(i_t=0) p(O_t^{\text{mz}} | K_t, i_t=0) \frac{(O_t^{\text{mz}} - \mu^{\text{mz}}(k))}{\sigma^2}}{p(O_t^{\text{mz}} | K_t)} \right) \\
&= \left( \prod_{t: K_t=k} p(O_t^{\text{mz}} | K_t) \right) \left( \sum_{t: K_t=k} p(i_t=0 | K_t, O_t^{\text{mz}}) \frac{(O_t^{\text{mz}} - \mu^{\text{mz}}(k))}{\sigma^2} \right).
\end{aligned}$$

$$\begin{aligned}
\Rightarrow \frac{\partial}{\partial \mu^{\text{mz}}(k)} \log p(s|x, \theta) &= \frac{1}{p(s|x, \theta)} \sum_{i_{1:T}, \delta_{1:T}} \mathbf{1}_{\{K_t=k\}} p(i_{1:T}, K_{1:T} | \theta) \sum_{t: K_t=k} p(i_t=0 | K_t, O_t^{\text{mz}}) \frac{(O_t^{\text{mz}} - \mu^{\text{mz}}(k))}{\sigma^2} \\
&= \frac{1}{p(s|x, \theta)} \sum_{t=1}^T p(i_t, K_t=k | \theta) p(i_t=0 | K_t, O_t^{\text{mz}}) \frac{(O_t^{\text{mz}} - \mu^{\text{mz}}(k))}{\sigma^2} \\
&= \sum_{t=1}^T p(i_t, K_t=k | s, \theta) p(i_t=0 | K_t, O_t^{\text{mz}}) \frac{(O_t^{\text{mz}} - \mu^{\text{mz}}(k))}{\sigma^2}, \tag{1}
\end{aligned}$$

where we equivalently write  $p(s|x, \theta) = p(i_{1:T}, \delta_{1:T} | \theta) = p(i_{1:T}, K_{1:T} | \theta)$  due to the deterministic relationship  $\delta_t = K_t - K_{t-1}$ .

## 3 Theseus Unsupervised Learning using Coordinate Ascent

Using the model’s Fisher scores, Theseus parameters  $\theta$  may be learned via maximum likelihood estimation. We present an alternate learning algorithm which we compare to maximum likeli-

---

**Algorithm 1** Unsupervised Learning in Theseus using Coordinate Ascent

---

```
1: while not converged do
2:   for  $i = 1, \dots, n$  do
3:      $\hat{x}^i \leftarrow \operatorname{argmax}_{x^i \in \mathcal{P}} \log p(s^i, x^i | \theta)$ 
4:   end for
5:    $\theta \leftarrow \operatorname{argmax}_{\theta} \sum_{i=1}^n \log p(s^i, \hat{x}^i | \theta)$ 
6: end while
```

---

hood learning in [2]. Let  $s^1, s^2, \dots, s^n$  be a dataset of spectra and define  $J(x^1, \dots, x^n, \theta) = \sum_{i=1}^n \log p(s^i, x^i | \theta)$ . Optimizing this objective function, Theseus' coordinate ascent learning algorithm is defined in Algorithm 1 where, rather than relying on training labels, we use max-product inference to infer the most probable PSM for each spectrum given the current iteration's parameters, then maximize the log-likelihood with respect to  $\theta$  given the most likely PSMs. We now prove that Algorithm 1 converges monotonically.

**Theorem 1.** *Algorithm 1 converges monotonically to a local optimum.*

*Proof.* We need to show that the objective function  $J$  is nondecreasing with each iteration of the algorithm. Denote the learned parameters at iteration  $k$  of the algorithm as  $\theta_k$  and define  $\hat{x}_k^i = \operatorname{argmax}_{x^i \in \mathcal{P}} \log p(s^i, x^i | \theta_{k-1})$ .  $\theta_k = \operatorname{argmax}_{\theta} J(\hat{x}_k^1, \dots, \hat{x}_k^n, \theta)$ . We thus have

$$\begin{aligned} J(\hat{x}_k^1, \dots, \hat{x}_k^n, \theta_k) &\geq J(\hat{x}_k^1, \dots, \hat{x}_k^n, \theta_{k-1}) \\ J(\hat{x}_k^1, \dots, \hat{x}_k^n, \theta_{k-1}) &\geq J(x^1, \dots, x^n, \theta_{k-1}), \forall x^1, \dots, x^n \in \mathcal{P} \\ \Rightarrow J(\hat{x}_k^1, \dots, \hat{x}_k^n, \theta_k) &\geq J(\hat{x}_{k-1}^1, \dots, \hat{x}_{k-1}^n, \theta_{k-1}) \end{aligned}$$

□

## 4 Impact of Recalibration over Standard DRIP Search

**Table 2:** Percent improvement over uncalibrated search results for the DRIP methods plotted in Figure 1, at an FDR threshold  $t = 1\%$ . Largest improvement highlighted in bold. Note that at this FDR threshold, Percolator post-processing using a standard set of features may result in diminished performance (Worm-3).

| Data set | DRIP | DRIP Heuristic | DRIP Fisher |
|----------|------|----------------|-------------|
| Yeast-1  | 5.4  | 10.7           | <b>14.8</b> |
| Yeast-2  | 5.2  | 8.3            | <b>16.6</b> |
| Yeast-3  | 9.2  | 10.9           | <b>17.7</b> |
| Yeast-4  | 3.4  | 7.5            | <b>15.1</b> |
| Worm-1   | 10.1 | 17.4           | <b>20.8</b> |
| Worm-2   | 1.1  | 6.7            | <b>11.3</b> |
| Worm-3   | -5.1 | 7.2            | <b>11</b>   |
| Worm-4   | 0.4  | 9.9            | <b>16</b>   |
| Average  | 3.7  | 9.8            | <b>15.4</b> |

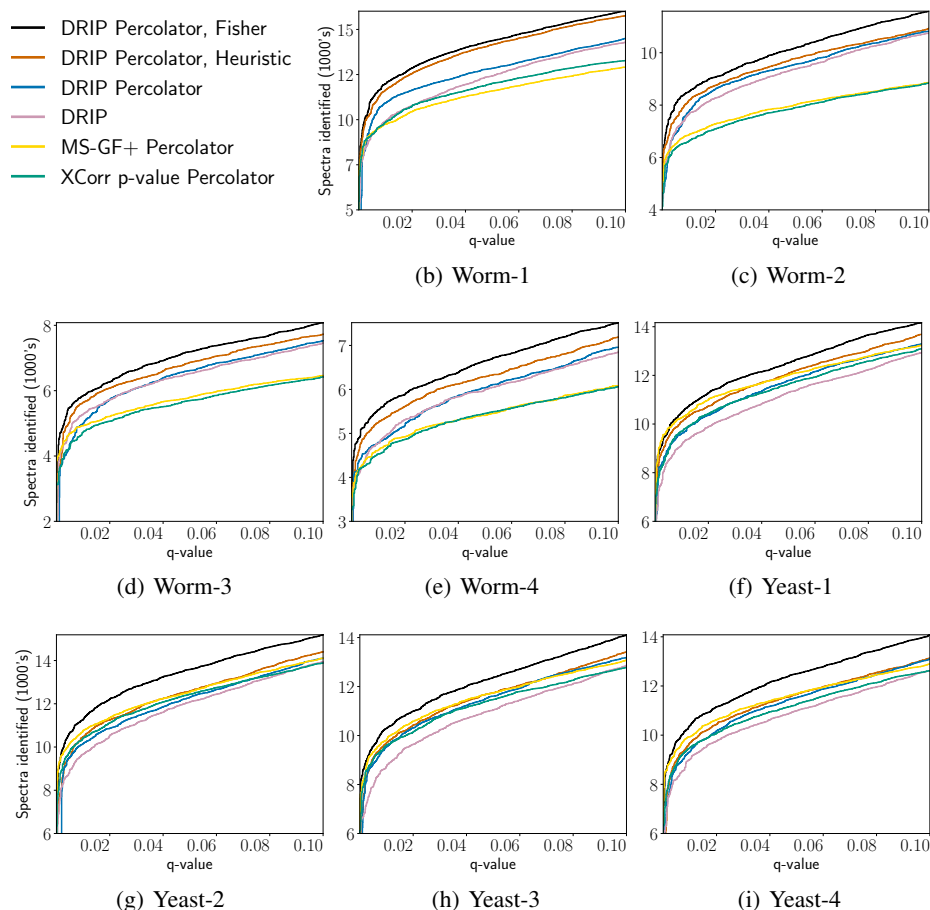


**Figure 1:** Performance increase of DRIP search after recalibration. Methods denoted by “Percolator” are post-processed using the Percolator SVM classifier [3], otherwise the raw PSM scores of the denoted search algorithm are used for identification. “DRIP Percolator” uses the standard set of DRIP PSM features described in [1], “DRIP Percolator, Heuristic” augments the standard set with DRIP-Viterbi-path parsed PSM features described in [1], and “DRIP Percolator, Fisher” augments the Heuristic set with the gradient-based DRIP features to the standard. XCorr  $p$ -value and MS-GF+ use their standard set of Percolator features, described in [1]. Search accuracy plots measured by  $q$ -value versus number of spectra identified for yeast (*Saccharomyces cerevisiae*) and worm (*C. elegans*) datasets.

## References

- [1] John T Halloran, Jeff A Bilmes, and William S Noble. Dynamic bayesian network for accurate detection of peptides from tandem mass spectra. *Journal of Proteome Research*, 15(8):2749–2759, 2016.
- [2] John T. Halloran and David M. Rocke. Gradients of Generative Models for Improved Discriminative Analysis of Tandem Mass Spectra. In *Advances in Neural Information Processing Systems*, July 2017.
- [3] L. Käll, J. Canterbury, J. Weston, W. S. Noble, and M. J. MacCoss. A semi-supervised machine learning technique for peptide identification from shotgun proteomics datasets. *Nature Methods*, 4:923–25, 2007.